

Selective acoustic phonon mode excitation of multi-mode silver nanoprisms

Po-Tse Tai^a, Pyng Yu^a, Jane Huang^a, Jau Tang^{a,b,*}

^a Research Center for Applied Sciences Academia Sinica, Taipei, Taiwan

^b Institute of Photonics, National Chiao-Tung University, Hsinchu, Taiwan

ARTICLE INFO

Article history:

Received 22 June 2010

In final form 20 July 2010

Available online 23 July 2010

ABSTRACT

Nanoprisms are known to exhibit two major planar phonon modes in ultrafast experiments, namely, a stronger mode related to the bisector height and a weaker mode related to half of the edge length. In this work we demonstrated photoacoustic excitation of a specific acoustic phonon mode in silver nanoprisms using two properly timed pump pulses. Using this technique, we could selectively excite only the weak totally symmetric mode while suppressing the dominant breathing mode. Via direct observation of such a mode, which is hardly detectable directly with the conventional single pump pulse technique, we could elucidate the roles of hot electrons in photoinduced ultrafast structural dynamics in laser-heated nanoparticles.

© 2010 Elsevier B.V. All rights reserved.

The investigation of laser heating and ultrafast structural dynamics of nanomaterials induced by a femtosecond laser pulse using optical pump–probe techniques or the ultrafast electron diffraction method has attracted much attention recently. The sudden heating of electrons and lattice by a femtosecond laser pulse induces impulsive thermal stress which causes the whole nanoparticle to vibrate. Usually, the oscillation period is proportional to the dimension of the object. The breathing mode exhibits an approximate period of $2L/v_s$, where v_s is the sound velocity and L is related to the nanoparticle size [1–11]. In some cases, higher order modes could be observed, such as in nanorods, nanocubes and nanoprisms [12–18].

Nanoprisms are known to exhibit two major planar phonon modes as shown in Fig. 1a and b. The first and dominant mode, often called the breathing mode, is related to the bisector height. The second but much weaker mode, often called the totally symmetric mode, is related to half of the side length. According to observation in the transient absorption experiments and simulation results [14–18], the detection of the totally symmetric mode is due to the width modulation of the plasmon resonance, and it is mainly caused by the peak-like impulsive electron stress. It means that the totally symmetric mode is difficult to be observed if the wavelength of the probe beam is far from the width of the plasmon resonance. In this work, we demonstrated the direct observation of the much weaker totally symmetric mode around the peak of the plasmon resonance by coherent control techniques when suppressing the more dominant breathing mode. This alternative ap-

proach with two properly timed pump pulses allows us to enhance detectable sensitivity of the totally symmetric mode and to improve the understanding of the hot-electron dynamics induced by laser heating.

In typical synthesis of silver nanoprisms, an aqueous solution of silver nitrate (0.1 mM), trisodium citrate (30 mM), poly(vinylpyrrolidone) (0.7 mM), and hydrogen peroxide (30%) were added in sequence at room temperature. Then, 100 mM sodium borohydride was injected into the mixture. Fig. 2a shows the UV–visible extinction spectra of nanoprisms formed under this condition. The dimension of the resulting silver nanoprisms with 43 ± 8.6 nm for the bisector and 7 ± 1.25 nm for the thickness was determined through the TEM image. The histogram of bisector is shown in the inset of Fig. 2b. Multiple pump beam configuration was used in this pump–probe experiment. The 100 fs laser pulse at 760 nm wavelength provided by a Ti:sapphire amplifier (Spifire, Spectra Physics, Inc.) with a repetition rate of 1 kHz was applied to the nanoprisms in single color pump–probe measurements. Here, the Spifire laser was pumped and seeded by a solid state laser (Empower, Spectra Physics, Inc.) and an oscillator of the Ti:sapphire laser (Tsunami, Spectra Physics, Inc.). Two motorized stages were used to control the delay time between two pump beams and one probe beam, which were irradiated on the sample with a pump/probe energy ratio of 100 to 1. The probed beam was detected by a photodiode detector (2001-FC, New Focus, Inc.), and the data signal was acquired by a personal computer through a lock-in amplifier (SR830, Stanford Research, Inc.). A perpendicular polarizer between the pump and probe beams was employed to minimize the influence from the pump beam scattered light. Here, the sample was circulated in a flow cell with 1 mm optical light path during the measurements.

* Corresponding author at: Research Center for Applied Sciences Academia Sinica, Taipei, Taiwan.

E-mail address: jautang@gate.sinica.edu.tw (J. Tang).

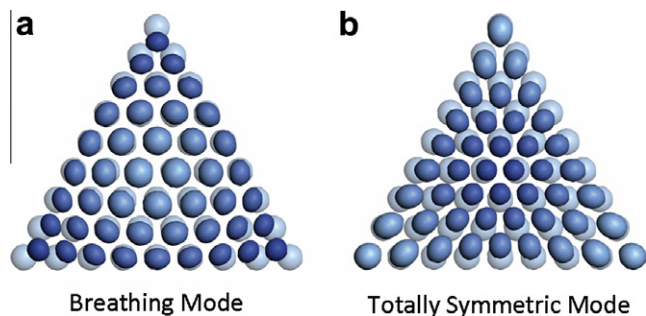


Fig. 1. (a) and (b) Schematic illustrations of two lowest vibrational modes in a triangular nanoprism, i.e., the breathing mode and the totally symmetric mode.

The transient absorption data for silver nanoprisms is shown in Fig. 3. The blue¹ curve represents the typical pump–probe result. The large peak that appears before 10 ps is due to photo-induced hot-electron dynamics, and the following damped sinusoidal oscillations are due to coherent acoustic phonons. We determined from the fitting an oscillation period T of 29.4 ± 0.05 ps. Using the approximate relation $T = 2h/v_s$ as reported by the Hartland's group [3] one could retrieve the bisector of nanoprisms. A slightly larger bisector of 53.6 nm than the mean of size distribution histogram was obtained by using the sound speed $v_s = 3650$ m/s. The overestimate of the size using the approximate relation was noted in previous studies using a variational approach to solve the elastodynamics problem [14,19].

In another recent study, by curve fitting to the oscillations with a single damped sinusoid, the residue of the fit showed a weak oscillatory component at a higher frequency which was identified as the totally symmetric mode [14]. Such an indirect method using the residue to determine high-order mode is not very robust and it could be susceptible to noise which has a magnitude on the order of the residue. To obtain a more accurate determination of the phase and the amplitude, we presented a better alternative using two properly delayed pump pulses to suppress the dominant breathing mode and to selectively excite the much weaker totally symmetric mode. In addition, this technique has been used by Del Fatti's group to detect a weak overtone mode for Ag nanospheres [7]. Two pump pulses were crossed on the BBO crystal to produce second harmonic generation and to determine the zero time delay. Then, the optical path was increased by 4.41 mm for the second pulse with a corresponding time delay of 14.7 ps with respect to the first pulse. This time delay was chosen to be equal to the half period of the breathing mode so that there would be destructive interference from the undesirable dominant mode. The experimental data are shown in Fig. 3a. The spikes represent the timing of the first pump pulse (P_1) and the second pump pulse (P_2). The extent of the suppression of the breathing mode could be controlled by adjusting the power of P_2 . As prescribed from the green curve in Fig. 3a, the oscillations are caused mainly by P_2 when the power of P_2 is larger than the power of P_1 . One could also clearly see that the green and blue curves are out of phase. Furthermore, the amplitude of the breathing mode decreases as the power of P_2 decreases. We have obtained an optimized condition when the power of P_2 was about one quarter of the power of P_1 . As shown from the red curve in Fig. 3a, the breathing mode was completely suppressed and the faster oscillations from the totally symmetric mode could be observed.

The oscillations from the totally symmetric mode displayed in Fig. 3b were fitted to $Ae^{-t/T_1} \sin(\omega t + \phi) + Be^{-t/T_2}$, where $\omega = 2\pi/T$

and T is the oscillation period. The amplitudes A and B , the damping time constants T_1 and T_2 , the angular frequency ω , and the initial phase ϕ were determined from the curve fitting. From the fitted oscillation period of $T \sim 18 \pm 0.08$ ps we found that the period of the breathing mode is about $\sqrt{3}$ times of that of the totally symmetric mode [14]. As shown in Fig. 3a from the comparison between the red and blue curves, the launching of the second pulse P_2 , which is properly delayed with respect to P_1 results in out-of-phase cancellation and suppression of the breathing mode. The success of such a scheme of selective excitation relies on proper choice of the pulse timing and power. Since the power of P_2 is four times weaker than the power of P_1 , this P_2 pulse only affects the totally symmetric mode slightly. In order to compare these two modes, we also used a damped sinusoid to fit the breathing mode of the blue curve in Fig. 3a. The initial phase difference between these two modes is 81° , with the initial phase of $148 \pm 3.4^\circ$ and $229 \pm 7.25^\circ$ for the breathing mode and the totally symmetric mode, respectively. Our experiment result regarding phase differences is consistent with previous studies [14–18].

Furthermore, here we discuss the dependence of the excitation power on coherent acoustic oscillations. As shown in Fig. 4a, the amplitude of the breathing mode depends on the excitation power which was varied from 0.5 to 2.3 $\mu\text{J}/\text{pulse}$. The magnitude of the modulations first increases with the pump power from 0.5 to 1.2 $\mu\text{J}/\text{pulse}$, but then decreases when the power is higher than 1.2 $\mu\text{J}/\text{pulse}$. We also observed another characteristic of the breathing mode, as the pump power increases the oscillation pattern shifts backward in time. Such behavior could be understood from the thermal heating mechanism of electrons and lattice as discussed in previous studies [8,20–25]. The dependence of the totally symmetric mode on pump power is shown in Fig. 4b. The shift of the oscillation pattern backward in time as the pump power increases is similar to the behavior of the breathing mode in Fig. 4a.

In a colloid sample of nanoparticles, the size of the nanoparticles is not homogeneous. Since the oscillation period depends on the particle size, a distribution of the sizes or the oscillation periods would contribute to the damping of the oscillations known as inhomogeneous broadening [20,26]. The yellow lines in Fig. 4 were fitted by the damped sinusoid as discussed previously with an invariant damping time of 25 ps for the totally symmetric mode and 45 ps for the breathing mode obtained. As shown from the green data dots in Fig. 4b, we also noticed that the magnitude of the totally symmetric mode drops suddenly when the excitation power exceeds 1.6 $\mu\text{J}/\text{pulse}$, and disappeared when the excitation power exceeded 2.3 $\mu\text{J}/\text{pulse}$. According to previous studies [8,27,28], non-uniformity or a gradient of electron temperature and lattice temperature inside a nanoparticle is essential in contributing to thermal stresses to drive acoustic vibrations. At a higher fluence, although the electron temperature increases, the electron thermal conductivity and the ballistic range also increase. The temperature gradient or thermal stress does not necessarily increase monotonically with laser fluence. These competing factors contribute to our experimental finding of an increase in the magnitude of the totally symmetric mode from the beginning, and then a decrease as the laser fluence gets higher. In addition, the tips of nanoprisms could be truncated at higher laser excitation intensity [29,30]. Unlike the ideal sharp tips, the snipped tips could cause a decrease in the optical absorption and a more uniform initial distribution of the electron temperature. Since the peak of SPR is sensitive to snipping [29,30], we could use the absorption spectrum to estimate the extent of snipped nanoprisms. At the maximum laser excitation, we found that the peak of SPR was blue-shifted by about 15 nm, indicating that the nanoprisms were snipped slightly.

In summary, in this study of photoacoustic excitation of silver nanoprisms, we used two properly timed laser pulses to control the selective excitation of the much weaker totally symmetric

¹ For interpretation of color in Figs. 3 and 4, the reader is referred to the web version of this article.

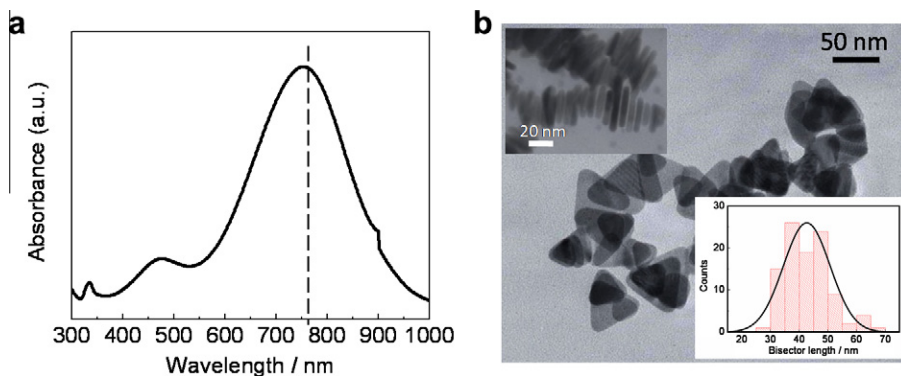


Fig. 2. (a) UV-visible spectra of the silver nanoprisms. The dashed line represents the wavelength of pump and probe beams. (b) The TEM image of the silver nanoprisms. Inset is the size distribution of the bisector height.

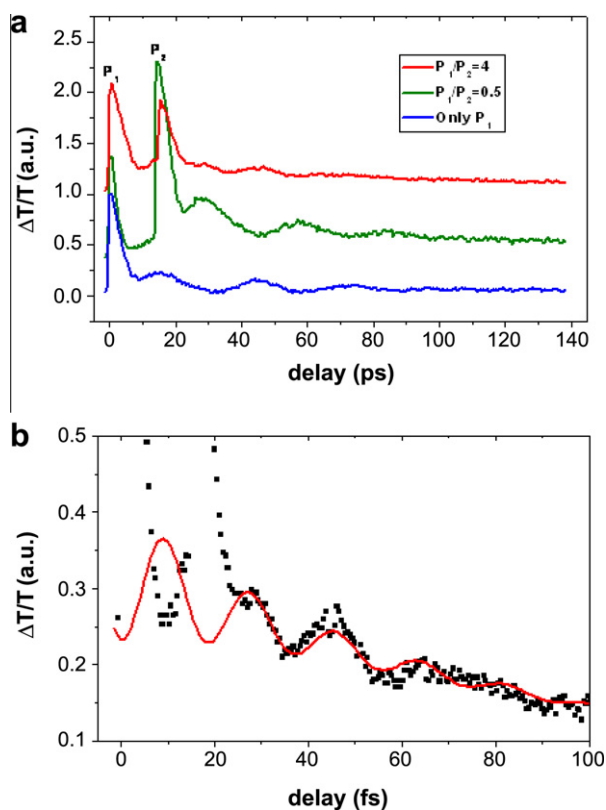


Fig. 3. (a) The observed transient absorption profiles with an excitation wavelength at 760 nm at a different pump power: $P_1 = 0.5 \mu\text{J}$ (blue line), $P_1/P_2 = 0.5$ (green line), and $P_1/P_2 = 4$ (red line), respectively. (b) Transmission changes of the totally symmetric mode on an enlarged scale. The red curve is fitted by a damped sinusoid with a period of 18 ± 0.15 ps. The data were normalized to peak signal near 0 ps.

mode while suppressing the fundamental breathing mode. In the usual pump–probe experiments with one single pump pulse, the presence of the dominant breathing mode is so strong that the second mode is hardly detectable. In the past, the much weaker totally symmetric mode was determined by extracting from the residue in curve fitting to overall transient data by one damped sinusoidal function. Such a numerical fitting approach is indirect and would not too reliable if S/N is poor. As an alternative, this coherent control technique allows us to observe such a weaker mode directly and to investigate its pump power dependence more rigorously. This approach could also be applied in photoacoustic excitation of nanoparticles with less symmetric shapes. The observation re-

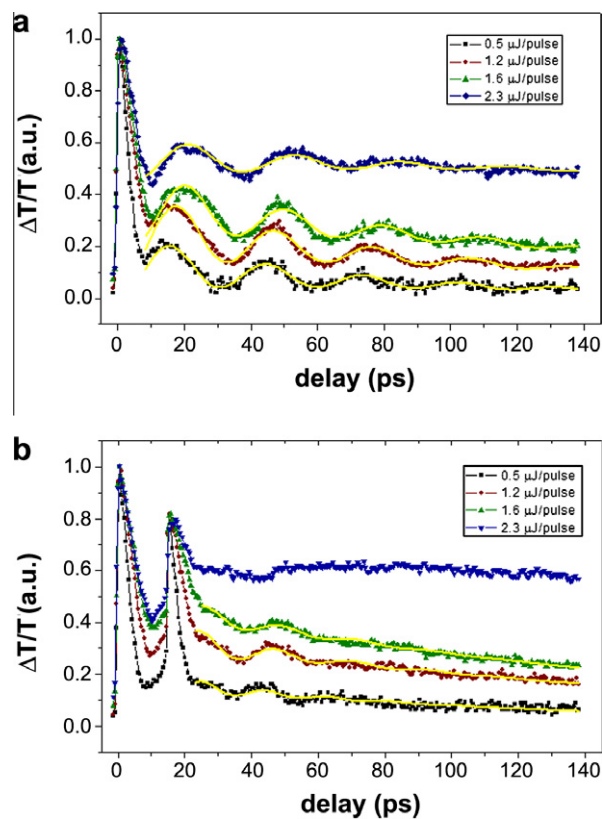


Fig. 4. (a) The pump power dependence with one pump pulse. (b) The pump power dependence with two properly timed pump pulses. The data were normalized to peak signal near 0 ps. The yellow line represents the fit by $Ae^{-t/T_1} \sin(\omega t + \phi) + Be^{-t/T_2}$.

ported here about the roles of hot electrons in ultrafast structural dynamics of nanoprisms is consistent with the descriptions of the two-temperature model that has been used by researchers to model hot-electron dynamics and electron thermal stresses induced by femtosecond laser heating.

Acknowledgment

J. Tang thanks the support of the Academia Sinica and National Science Council (NSC) of Taiwan under the program No. 98-2221-E-001-019. P.T. Tai and P. Yu acknowledge NSC and AS for providing postdoctoral fellowship.

References

- [1] A.H. Zewail, *Annu. Rev. Phys. Chem.* 57 (2006) 65.
- [2] J. Tang, D.S. Yang, A.H. Zewail, *J. Phys. Chem. C* 111 (2007) 8957.
- [3] M. Hu, H. Petrova, X. Wang, G.V. Hartland, *J. Phys. Chem. B* 109 (2005) 14426.
- [4] W. Huang, W. Qian, M.A. El-Sayed, *J. Phys. Chem. B* 109 (2005) 18881.
- [5] C. Voisin, N. Del Fatti, D. Christofilos, F. Vallee, *J. Phys. Chem. B* 105 (2001) 2264.
- [6] C. Voisin, N. Del Fatti, D. Christofilos, F. Vallee, *Appl. Surf. Sci.* 164 (2000) 131.
- [7] A. Arbouet, N. Del Fatti, F. Vallee, *J. Chem. Phys.* 124 (2006) 144701.
- [8] P.T. Tai, P. Yu, J. Tang, *J. Phys. Chem. C* 113 (2009) 15014.
- [9] G.V. Hartland, *Phys. Chem. Chem. Phys.* 6 (2004) 5263.
- [10] M. Perner, S. Gresillon, J. Marz, G. Von Plessen, J. Feldmann, *Phys. Rev. Lett.* 85 (2000) 792.
- [11] N. Del Fatti, C. Voisin, D. Christofilos, F. Vallee, C. Flytzanis, *J. Phys. Chem. A* 104 (2000) 4321.
- [12] H. Petrova et al., *J. Chem. Phys.* 126 (2007) 094709.
- [13] M. Hu, X. Wang, G.V. Hartland, P. Mulvany, J.P. Juste, J.E. Sader, *J. Am. Chem. Soc.* 125 (2003) 14925.
- [14] L. Bonacina, A. Callegari, C. Bonati, F.V. Mourik, M. Chergui, *Nano Lett.* 6 (2006) 7.
- [15] R. Zadoyan, H. Ye Seferyan, A.W. Wark, R.M. Corn, V.A. Apkarian, *J. Phys. Chem. C* 111 (2007) 10836.
- [16] N. Del Fatti, C. Voisin, F. Vallee, C. Flytzanis, *J. Chem. Phys.* 110 (1999) 11484.
- [17] P. Yu, J. Tang, S.H. Lin, *J. Phys. Chem. C* 112 (2008) 17133.
- [18] P.T. Tai, J. Tang, *J. Sci. Conf. Proc.* 1 (2009) 207.
- [19] J. Burgin, P. Langot, N. Del Fatti, F. Vallee, W. Huang, M.A. El-Sayed, *J. Phys. Chem. C* 112 (2008) 11231.
- [20] J.H. Hodak, A. Henglein, G.V. Hartland, *J. Phys. Chem. B* 104 (2000) 9954.
- [21] J.H. Hodak, A. Henglein, G.V. Hartland, *J. Chem. Phys.* 111 (1999) 8613.
- [22] J. Wang, C. Guo, *Phys. Rev. B* 75 (2007) 184304.
- [23] J. Tang, *J. Chem. Phys.* 128 (2008) 164702.
- [24] J. Tang, *Appl. Phys. Lett.* 92 (2008) 011901.
- [25] G.V. Hartland, M. Hu, J.E. Sader, *J. Phys. Chem. B* 107 (2003) 7472.
- [26] P. Zijlstra, A.L. Tchegotareva, J.W.M. Chon, M. Gu, M. Orrit, *Nano Lett.* 8 (2008) 3493.
- [27] O.B. Wright, *Phys. Rev. B* 49 (1994) 9985.
- [28] J.K. Chen, J.E. Beraun, L.E. Grimes, D.Y. Tzou, *Int. J. Solids Struct.* 39 (2002) 3199.
- [29] K.L. Kelly, E. Coronado, L.L. Zhao, G.C. Schatz, *J. Phys. Chem. B* 107 (2003) 668.
- [30] Q. Zhang, J. Ge, T. Pham, J. Goebel, Y. Hu, Z. Lu, Y. Yin, *Angew. Chem. Int. Ed.* 48 (2009) 3516.